DEVELOPMENT OF A NEW METHOD TO MEASURE THE CREEP BEHAVIOR OF RUBBER WITH THE ADDITION OF BENTONITE BASED ON SCANNER-BASED IMAGE PROCESSING

By:

TAN WAI YEE

(Matrix no.: 125430)

Supervisor:

Professor Dr. Mani Maran Ratnam

May 2018

This dissertation is submitted to
Universiti Sains Malaysia
As partial fulfilment of the requirement to graduate with honors degrees in
BACHELOR OF ENGINEERING
(MANUFACTURING ENGINEERING WITH MANAGEMENT)

School of Mechanical Engineering
Engineering Campus
Universiti Sains Malaysia

DECLARATION

This work has not previously been accepted in substance for any degree and is not being concurrently in candidature for any degree.

Signed ……..….…..... (TAN WAI YEE)

Date……..….…..…..

STATEMENT 1

This thesis is the result of my own investigations, except where otherwise stated. Other sources are acknowledged by giving explicit references. Bibliography/references are appended.

Signed ……..….…..... (TAN WAI YEE)

Date……..….…..…..

STATEMENT 2

I hereby give consent for my thesis, if accepted, to be available for photocopying and for interlibrary loan, and for the title and summary to be made available outside organizations.

Signed ……..….…..... (TAN WAI YEE)

Date……..….…..…..

Witness by

Supervisor: Professor Dr. Mani Maran Ratnam

Signed ……..….…..…..

Date……..….…..…..

ACKNOWLEDGEMENT

My project would not have completed without the aid and support from various parties. First and foremost, I would like to extend my greatest gratitude to my supervisor, Prof. Mani Maran Ratnam for his continuous assistance and guidance given throughout the whole project process. I also would like to thank my supervisor for his unconditional support and valuable information which cleared my doubts and leaded me to the right direction.

Besides that, I would like to express my highest appreciation to technicians of School of Mechanical Engineering who have gave good suggestions to me based on their experience in fabrication and parameters setting for machines. These helped me to avoid using wrong method and settings which eliminated repetitive experiments due to failure.

Similarly, I am grateful to Professor Dr. Hanafi Ismail and Mr Amin Ibnu Lotfi from School of Materials & Mineral Resources Engineering who have prepared rubber specimens for me. With their help, I have specimens ready for me to carry out my project.

In addition, I would like to thank my course mates and friends who have gave comments, suggestions and encouragement to allow me generated more ideas and be more positive throughout this journey of completion of work.

Last but not least, I would like to appreciate all who have directly or indirectly supported me throughout this project.

TABLE OF CONTENTS

LIST OF TABLES

Tables **Title** **Page**

LIST OF FIGURES

Figure **Title** **Page**

LIST OF ABBREVIATIONS

Abbreviations	Representation
DIC	Digital Image Correlation
3D	Three dimensional
NR	Natural rubber
SBR	Styrene-butadiene rubber
NBR	Nitrile-butadiene-rubber
EPDM	Ethylene propylene diene rubber
MMT	Montmorillonite
CCD	Charged coupled devices
phr	parts per hundred rubber
CB	Carbon black

ABSTRAK

Ujian rayapan adalah penting untuk menentukan jumlah ketegangan yang dapat ditahan oleh spesimen di bawah tekanan untuk mengenal pasti kesesuaian bahan tersebut untuk sesuatu aplikasi. Beberapa kaedah telah diguna untuk mengukur rayapan getah seperti alat pengukur rayapan tegangan unisikal, korelasi imej digital (DIC) dan melalui penilaian oleh 3D Neural Network Reconstructor menggunakan ujian bulge. Tujuan penyelidikan ini adalah untuk mencipta kaedah baru untuk mengukur rayapan getah dengan penambahan bentonit pelbagai pemuatan berdasarkan kaedah pemprosesan imej berasaskan pengimbas. Penutup telah dibuat dan penanda dicipta pada spesimen getah. Pengimbas flatbed digunakan untuk pemerolehan imej. Faktor skala adalah 0.0423 mm/piksel. Ujian pengesahan dijalankan untuk memastikan algoritma MATLAB yang diguna adalah tepat. Spacers yang digunakan untuk memberi ketegangan semasa ujian pengesahan telah disediakan. Nilai terikan yang diukur dibandingkan dengan nilai terikan yang diguna untuk menentukan ralat peratusan. Persamaan penentukuran dimasukkan dalam algoritma untuk menghapuskan ralat sistematik. Ujian tegangan dijalankan untuk menentukan beban yang sesuai untuk digunakan semasa ujian rayap. Ujian rayap dijalankan pada spesimen getah dengan beban bentonit yang berlainan (0, 10, 30, 50 dan 70 phr). Keputusan menunjukkan bahawa beban bentonit meningkatkan rintangan rayap spesimen getah. Dapatan kajian ini menunjukkan keupayaan kaedah yang dicipta untuk mengkaji kelakuan getah berdasarkan kaedah pemprosesan imej berasaskan pengimbas.

ABSTRACT

Creep test is important to determine the amount of strain a specimen can withstand under pressure to identify the suitability of this material to certain application. There are several methods that are used to measure rubber creep such as uniaxial tensile creep measurement apparatus, digital image correlation (DIC) and through the assessment by a 3D Neural Network Reconstructor using bulge testing. The purpose of this research is to develop a new method to measure the creep behavior of rubber with the addition of bentonite of various loading based on scanner-based image processing method. A mask was fabricated and markers were created on the gage length of rubber specimen. A flatbed scanner was used for image acquisition. The scale factor is 0.0423 mm/pixel. A validation experiment was carried out to ensure that the MATLAB algorithm developed is accurate. Spacers used to apply strain during validation test were prepared. The measured strain values were compared with the applied strain values to determine the percentage error. Calibration equations were inserted in the algorithm to remove systematic error. Tensile test was carried out to determine the suitable constant load that should be applied during creep test. Lastly, the creep test was carried out on rubber specimen with different bentonite loadings (0, 10, 30, 50 and 70 phr). The results show that bentonite loading increases the creep resistance of rubber specimen. The findings from this research indicated the capability of the method developed to investigate the creep behavior of rubber based on scanner-based image processing method.

CHAPTER 1
INTRODUCTION

1.1 Background

In the current rubber research, there are large number of natural rubber (NR) and synthetic rubbers such as styrene-butadiene rubber (SBR), nitrile-butadiene-rubber (NBR) and ethylene propylene diene rubber (EPDM) which are added with reinforcing fillers to achieve the desired properties for products. There are black fillers and white fillers. Carbon blacks are black fillers, also known as the primary rubber reinforcing fillers. An example of white fillers is precipitated amorphous silicas. Reinforcing white fillers are effective in rubber formulations to add tear strength, abrasion resistance, and aging resistance to rubber products. Maria et al. (2014) said that it is important to have reinforced material so that rubber products can have longer life time and reduce material consumption.

One type of reinforcing material for rubber is bentonite. Bentonite is an absorbent aluminium phyllosilicate clay that consists mostly of montmorillonite (MMT). It has a wide range of applications. In the rubber industry, bentonite is an effective anti-tack for rubber extrusion in tire manufacturing process. Other than that, it provides earthing for underground cables to prevent them from corroding by lowering the soil resistivity. Bentonite is also used in other applications such as mud constituent for oil and water well drilling, binding agent in the production of iron ore pellets, lubricant agent in diaphragm walls and foundations for construction and others.

Since bentonite is used in rubber tire manufacturing, its creep property is a characteristic that should be determined. Creep is the tendency of a material after being subjected to high levels of stress, to change its form in relation to time. Creep test is important to determine the amount of strain or load a specimen can withstand under pressure to identify the suitability of this material to certain application. It also can determine the stability of a material and its behavior when it is put through normal stresses. Theoretically, creep increases with temperature and it is even more significant when a material is exposed to high temperature, which is at its melting point for a long period.

The suitable amount of bentonite to be added as reinforcing agent might be different for different rubber products. Therefore, the effect of amount of bentonite loading for creep test should be determined by preparing specimens with different bentonite loadings, which is applicable to real life situation.

There are several methods that are known to be used to measure creep test. Firstly, it is through uniaxial tensile creep measurement apparatus where a specimen is fixed in mechanical grips and stress is applied. There is an optical extensometer attached to the specimen. Other than that, another method is digital image correlation, which is used for creep compliance test. In this method, a specimen is gripped using a holder at the top and load is gently and manually applied to the bottom. There are two black and white charged coupled devices (CCD) cameras mounted on a tripod and connected to a computer to log the frames taken. Moreover, creep of hyperelastic material can be assessed by a 3D Neural Network Reconstructor using bulge testing. A pressure regulator is used to ensure constant pressure, which is essential for creep. From the creep measurement methods described above, there are some improvement opportunities that can be observed. Therefore, a different method, which is using scanner-based image processing method can be considered to determine the creep of rubber specimen.

Image processing especially digital image processing applies various methods or different algorithms to carry out require tasks. In the preprocess stage, it can remove noise, remove non-uniform background, improve contrast, remove blobs and sharpen the digital images. By using image processing method, the strain due to deformation of rubber specimen can be easily detected by having markers created on its gage length beforehand. These markers will deform together with the specimen during creep. Thus, the strain can be measured by detecting the distance between the markers.

Scanner-based image processing is the use of a CCD flatbed scanner to replace CCD cameras for image acquisition. According to Goh et al. (2016), flatbed scanner uses a single array of photo sensors and is capable of acquiring images at high resolutions over a large area deformation. The built-in lighting in the scanner offers a significant advantage over the conventional DIC setup as there is no external lighting needed. These advantages solve the frequently occurred problems of out of the field-of-view of the camera and low image resolution as well as introduces optical distortions.

1.2 Problem Statement

The several methods used to measure creep properties of rubber specimen can be improved. Firstly, electronic digital caliper is used to measure the distance between bench marks. This needs to be done manually thus its accuracy is doubted and can be improved. Then, extensometer is used to replace digital caliper, but this requires additional setup for extensometer to measure the strain during the test. This causes higher cost and more setup time is needed. Besides that, the method to measure strain using DIC optical method has high reliability in application, but this method needs to develop complicated algorithm and it takes long time to process. In addition, two CCD cameras are needed to mount on the setup. This increases the expenses too. Therefore, a simple scanner-based image processing method is developed to detect the markers created on the specimen and measure the distance between them to get the strain measurement.

1.3 Objective

The objective of this research is to develop a new method to investigate the creep behavior of rubber with the addition of bentonite of various loading based on scanner-based image processing method.

1.4 Scope of Work

The information on the method to measure creep properties of rubber with the addition of fillers and scanner-based image processing method are gathered. Next, a mask is fabricated to expose only certain regions at the gage length of a specimen to the black spray paint. The mask fabricated is used to put on specimen to create markers for gage length detection. Then, images are acquired by using flatbed scanner.

After that, validation experiment is carried out to ensure the accuracy of the MATLAB algorithm developed. The measured strain results are compared with the applied strain. The algorithm is improved until the percentage error is within 1%.

Next, a tensile test is carried out on five specimens with different bentonite loadings using Instron 3367 machine. This is to determine the maximum load and maximum strain of the specimens before fracture. Then, creep tests are carried out on the five different loading

specimens. The experimental setup is done according to standard test specifications for rubber. An optimum load is chosen and the load applied to all the five specimens is constant. The results obtained are analyzed to observe and compare the rubber creep rate of specimens with different bentonite loading.

CHAPTER 2
LITERATURE REVIEW

2.1 Introduction

This chapter reviews published journals on different types of filler added in rubber to identify the changes and effect in their properties. Besides that, the review on different methods used to carry out creep test on rubber specimen is done to acknowledge the current methods used and determine the opportunity and possibility to develop a better method. Several literatures on rubber creep test are studied to have a better understanding on the standard procedures used and expected results on creep test. The usage and its benefits of using scanner-based image processing method are studied to implement it in this research.

2.2 Filled Rubber

Rubber is added with fillers which can be used as reinforcing agents to alter and get desired properties of composites. Fillers are particles added into different types of material such as rubber, plastics and composites, to lower the consumption of more expensive binder material or to obtain better properties. There are two main types of reinforcing fillers for rubber which are carbon black and amorphous silica. Fillers in rubber are important to achieve longer lifespan of products, increase tire strength and especially for silica, it decreases the amount of greenhouse gases emission of the vehicles using these tires.

According to Wu et al. (2007), rubber with montmorillonite (MMT) nanocomposites possess the best flame retardance, such as lower peak heat release rate and higher fire performance index value. Mat et al. (2016) studied the bentonite filled ethylene propylene diene rubber (EPDM) composite and they found that the maximum torque of composite decreases at high bentonite loading. In addition, the tear strength of composite increased with increase in bentonite loading up to 90 phr (parts per hundred rubber) due to a better dispersion of bentonite clay. Zhang and Wang (2017) showed that compounding of NR and dendrimer modified flame-retardant organic montmorillonite with loading of 20 phr (FR-DOMt-20) composite possesses the highest tensile strength and this is resulted from complicated interactions between layered silicates and elastomers.

Ramadhan et al. (2015) concluded in their research that bentonite has great prospects to be used as filler in natural rubber industry after either physical or chemical process modification, such as reduction of its mineral impurities and upgrade bentonite to form organo-bentonite by addition of commercially available surfactant. Gu et al. (2009) investigated the mechanical properties, thermal stability and swelling behavior of SBR/NR/organo-bentonite nanocomposite. The addition of a small amount of organo-MMT improved its thermal stability and swelling behavior greatly, which is attributed to the good barrier properties of the dispersed and partially exfoliated organo-MMT particles.

El-Nashar et al. (2012) used ion exchange bentonites (IEBs) as fillers in SBR composites. The natural bentonite containing Na and Ca was cationically exchanged with Ba, Sr, Cu and Cu–Ba. Different loadings of IEBs were incorporated in SBR matrix to study their effect as reinforcing filler in rheometric characteristics, physico-mechanical properties and swelling. The results revealed that the performances of Ba- and Sr-bentonites are the best with an optimum loading at 15 phr. Cu bentonite showed the least performance, while addition of Cu to Ba deteriorated the reinforcing efficiency of Ba.

Chakraborty et al. (2010) used in-situ sodium activated organo modified bentonite clay to partially replace carbon black (N330). The study revealed that with slight modification of the curing package, up to 10 phr of the carbon black is possible to be replaced. At equivalent loading of 5 and 10 phr of in-situ sodium activated organo modified bentonite clay exhibited better properties as compared to carbon black filled compound. Pajtášová et al. (2017) prepared rubber compounds with bentonite as fillers. The vulcanizates were evaluated for their physical and mechanical properties such as tensile strength, elongation and hardness. These characteristics were compared with standard filler carbon black of N339 type, which is typical for standard rubber compounds used in the rubber industry.

Maria et al. (2014) studied the stress relaxation behaviour of NR/NBR nanocomposite vulcanite, reinforced with two different organically modified clay, which were MMT modified with dimethyl, benzyl, HT and another one was MMT modified with mercapto silane. The effects of loading, blend composition, filler polarity and temperature on stress relaxation of the reinforced nanocomposites were measured. Garishin et al. (2017) used carbon black, MMT and expanded MMT by stages to identify how each of these reinforcing agents modify the

properties of the elastomeric nanocomposites. The elastomers were tested for their mechanical properties, which were monotonic uniaxial stretching before fracture and cyclic uniaxial deformation.

Ghoreishy et al. (2014) prepared two series of passenger car tire rubber compounds reinforced with different carbon black types and loadings. Single type filler was used in the first series while blend of two carbon black types was employed in the second series. There were four types of carbon black with different particle size and structure, including N220 (lowest particle size), N330, N375 and N550 (highest particle size). The total carbon black volume in all compounds were kept constant and equaled to 60 phr.

From all these researches, the results show that addition of filler in rubber changed the properties of the main material and they are able to obtain desired characteristics in the newly formed composites.

2.3 Methods to Measure Creep Behaviour of Filled Rubber

There are several methods used to carry out creep test. Oman and Nagode (2014) carried out creep test at room temperature. For the uniaxial tensile creep test, a specimen was fixed in mechanical grips and then pre-stressed to 0.1MPa to obtain a flat specimen. Then, an optical extensometer was attached to the specimen and the nominal force sensor was set to zero. After the desired stress or strain was applied, the nominal travel sensor was set to zero and the measurement started. The duration of the test was 1800 seconds. The creep was measured at three different stress levels (5, 7.5 and 10MPa). The creep test results are as shown in Figure 2.1. The opportunity for improvement in this method is to eliminate the need to use an extensometer as it requires additional setup.

Mostafa et al. (2009) carried out creep test according to ASTM D 674 standard under three loading levels. The results of five different compositions with 0, 20, 30, 50 and 70 phr of carbon black (CB) loadings were compared and it was found that the creep resistance increases as CB loading increased. An example of creep strain for reinforced NBR vulcanizates at 1.68MPa stress level is shown in Figure 2.2. The limitation in this research is that the distance between the bench marks is measured manually by using electronic digital caliper with 0.01 mm accuracy. The accuracy of the measured distance is doubted and can be improved.

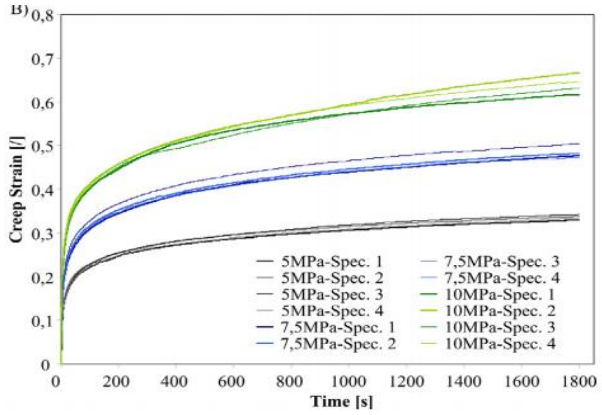

Figure 2.1: The graph of creep strain against time for specimen applied with three different stress levels (5, 7.5 and 10MPa). (Oman and Nagode, 2014)

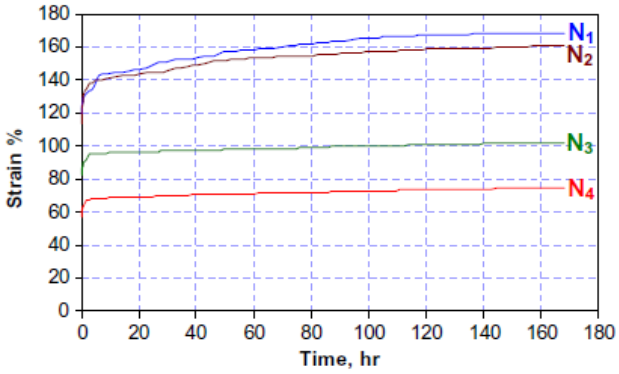

Figure 2.2: The variation of creep strain versus time for NBR vulcanizates with CB loading under 1.68MPa stress level. (Mostafa et al., 2009)

Siengchin and Karger-Kocsis (2009) carried out short time creep tests in tensile mode at different temperatures using dynamic mechanical analysis apparatus. The creep compliance was determined as a function of the time for 60 min. The temperature set was 40°C. The tensile stress applied was 5MPa. The temperature dependence of the creep response of the polyamide-6 and its composites was also studied, which is in the range from -75 to 75°C. The duration for this creep test was 15 minutes.

Dinh et al. (2015) used digital image correlation (DIC) for small strain measurement in deformable solids and geomechanical structures. DIC is a well-known contact-less technique offering highly accurate full-field deformation measurement using grayscale images. By tracking and comparing progressive images, strain can be mapped across the surface. This

allows the determination of displacements and reconstruction of strains. The general setup for DIC is as shown in Figure 2.3.

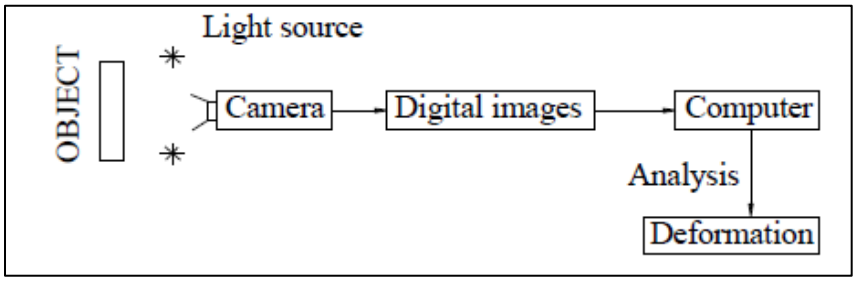

Figure 2.3: The general DIC setup. (Dinh et al., 2015)

Gu (2015) showed the basic principle of the standard subset-based DIC, which is shown in Figure 2.4. A square subset of N × N pixels surround the tested points in the reference image is selected and used to find its corresponding location in the deformed image by defining the maximum value of the calculated correlation coefficient. The vector between the reference subset center and target subset center is the in-plane displacement vector at the interested point P(x, y). A correlation coefficient distribution is acquired by moving the reference subset through the searching subset and calculating the correlation coefficient at each location.

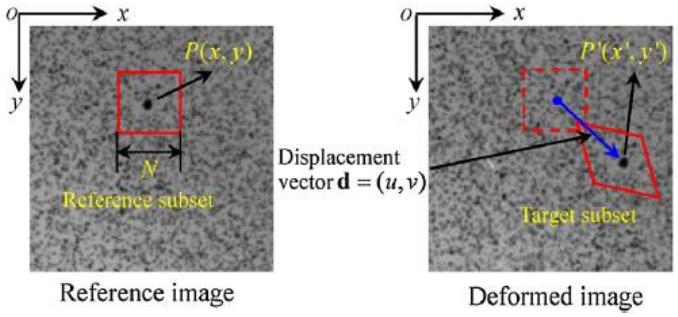

Figure 2.4: Schematic of relation of pixel point in reference and deformed subsets. (Gu, 2015)

Farfán-Cabrera et al. (2018) determined the creep degradation of sealing elastomers due to exposure to fluids using DIC. The specimens were finely speckled with white paint. A specimen was gripped at the top using a holder, which was mounted on a precision loading frame, as shown in Figure 2.5. The load is gently and manually applied to the bottom to generate the required constant load for creep test. A blinder clip is used to grip the dead weight to the specimen to produce axial strength. The DIC equipment (Dantec Dynamics Q-400system) was employed to measure the strains and displacements generated in the specimen in real time.

The equipment consists of two black and white CCD cameras that are mounted on a high precision tripod and connected to a computer to log the frames taken. A white light source was used to illuminate the specimen. This short creep experiment was conducted for 3 hours under a tensile load of 1.5N at room temperature of 25°C.

One of the disadvantages in DIC method is that it requires to develop complicated algorithm to calculate the correlation coefficient between the reference and deformed image at each location. The processing time for DIC is long too. Besides that, the need to have DIC equipment with two CCD cameras is costly. Similarly, additional setup for white light source is needed for illumination of the specimen.

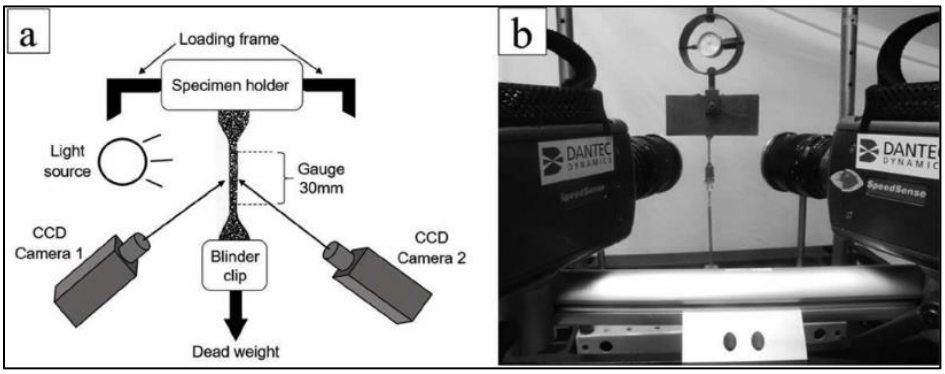

Figure 2.5: (a) Schematic view of the creep test setup and (b) photography of the creep test setup and DIC equipment. (Farfán-Cabrera et al., 2017)

Lo Savio et al. (2017) developed a new methodology based on Neural Network approach for three-dimensional reconstruction of pseudo-hemispherical geometry of a hyperelastic specimen during a creep bulge test. The experimental setup consists of two main elements, which are chamber for the bulge test with a pneumatic inflation system and a sliding crossbar that supports two cameras for tracking material deformation, as shown in Figure 2.6. The size of the captured images by the fixed-focus cameras is exclusively due to the dome deformation and not to the lens distance. Moreover, it is possible to ensure a sufficient depth of field which is very small at such short distances. A creep test was performed by insufflating air into the chamber as quickly as possible until a desired pressure (75 kPa) was reached. The constant pressure is maintained inside the bulge chamber by the pressure regulator. During the transient phase, the cameras acquire images at a frequency of 30 Hz. During the relaxation phase, the frequency is at 0.033 Hz (2 images/min).

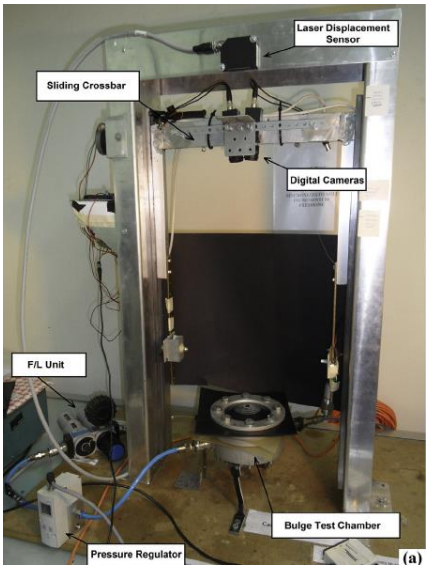

Figure 2.6: The experimental setup consists of the frame with sliding crossbar. (Lo Savio et al., 2017)

2.4 Scanner-based Digital Image Correlation

Goh et al. (2016) used scanner-based DIC (SB-DIC) method to determine the full-field in-plane displacement as well as the Young's modulus of elastomeric material up to 350%. A low-cost CCD flatbed scanner was used as the image acquisition device instead of digital cameras as in the conventional DIC method. This is because there are a lot of limitations in the conventional DIC method when applied to high-strain materials, such as polymer and rubber. The large deformation will cause the domain under study to go out of the field-of-view of the camera. The mounting of camera on an elevation stage for translation during the loading limited to about 15 x 5 mm at resolution of 4096 x 1400 pixels. The use of camera lens of a shorter focal length can overcome the limited field-of-view of camera, but the image resolution will be reduced and optical distortions might occur. Therefore, SB-DIC is an effective solution.

Besides that, Goh et al. (2017) studied the single-step SB-DIC method and compared it with incremental SB-DIC method. Incremental SB-DIC method is prone to cumulative errors since the total displacement is determined by combining the displacements in numerous stages of the deformation. On the other hand, with single-step SB-DIC method, the results show that it can map strain distribution accurately in large deformation materials like rubber at much shorter time compared to the incremental SB-DIC method.

In conclusion, DIC is used to measure localized strain. If total strain is needed instead of localized strain, a better method is to measure the strain based on gage length by using simple digital image processing method such as distance measurement. However, the use of flatbed scanner to acquire images is a good method. This is because it is capable of acquiring images at high resolutions over a large area. Similarly, it has built-in lighting in the scanner. Therefore, scanner-based image acquiring method will be employed in this research.

2.5 Summary

After reviewing previous works, it is found that bentonite is frequently used as the reinforcing filler in researches to explore its opportunity to obtain the desire properties for composites. Bentonite increases the flame retardance, tear strength and tensile strength of rubber composite. Other than that, methods to measure rubber creep are determined. Uniaxial tensile creep test method has a limitation that the accuracy of the measured distance is doubted and can be improved. Although DIC method is well-known for high accuracy in small strain measurement, it has a limitation that complicated algorithm is required to be developed and the processing time is long too. Another method identified is by using Neural Network approach for 3D reconstruction of pseudo-hemispherical geometry of a hyperelastic specimen during a creep bulge test. In addition, scanner-based image acquiring method will be employed in this research as flatbed scanner is capable of acquiring images at high resolutions over a large area and has built-in lighting.

CHAPTER 3
RESEARCH METHODOLOGY

3.1 Introduction

This chapter explains the methods used to complete this research. It includes the mask fabrication, markers creation, development of image processing algorithm, validation experiment, stress-strain test and creep test. The procedures involved in each subsection were described and illustrated clearly.

3.2 Fabrication of Mask

A mask was fabricated to ease the creation of markers at the gage length of specimen. The centroid of the markers was created at the gage length accurately and consistently. The dimensions of the mask are as shown in Figure 3.1. There are two similar masks fabricated as shown in Figure 3.2.

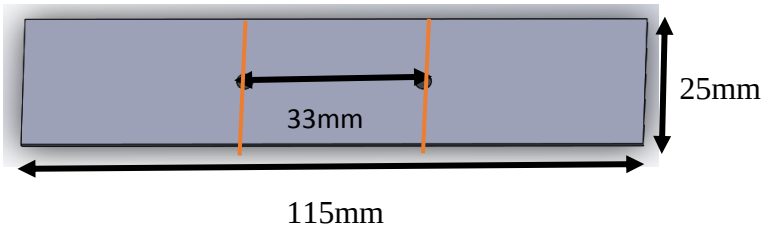

Figure 3.1: The dimensions of the mask.

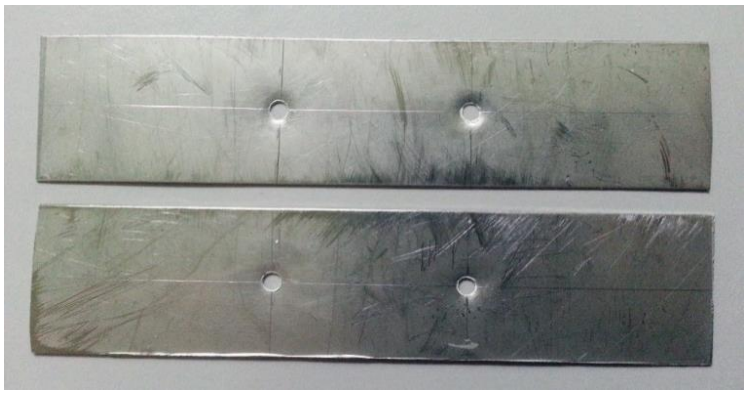

Figure 3.2: Two masks were fabricated.

3.3 Creation of Markers on Rubber Specimen

Several methods were tried to create markers on the rubber specimen. The first few methods, such as using liquid paper, general-purpose latex glue and shoes glue, as shown in Figure 3.3 and 3.4, failed to create markers that will deform together with the specimen as it is stretched. However, the markers created using the last method, Method 3, are acceptable.

Figure 3.3: Marker created using general purpose latex glue.

(a)  (b) 

Figure 3.4: Markers created using different brands of shoes glue, (a) x'traseal and (b) Original.

The first method, Method 1 failed. This method in which the mixing of a small amount of white poster colour together with rubber glue then pouring the mixture onto the specimen covered with the mask. But there is a reason that caused the failure, which is the mixture will stick on the mask instead of the specimen. Therefore, when the mask was removed, there were no markers created on the gage length. If without using the mask, a non-consistent shape of marker was created, which is as shown in Figure 3.5.

The second method, Method 2 also failed. In this method, the white poster colour was painted in thin layer on the gage length of specimen covered with mask first, then the mask was removed. After that, a layer of rubber glue was applied to function as a protective layer to the white poster colour, as shown in Figure 3.6. The failure reason of this method is that the

rubber glue protective layer will harden and peel off when it was stretched after few days the markers were created. Therefore, a better method that will produce uniform, consistent and long-lasting markers is needed.

Figure 3.5: Inconsistent shape of marker was formed.

(a)  (b) 

Figure 3.6: Different shapes of markers, (a) rectangular and (b) circle, were created with a rubber glue protective layer that will harden and peel off.

The third method (Method 3), which is the successful method is by using spray paint to spray speckle on the gage length of specimen covered with mask. Previously, spray paint method was used before but it was sprayed thoroughly instead of just creating a speckle pattern. Therefore, the paint will harden and peel off when the specimen was stretched.

In Method 3, firstly, a specimen was put on the floor flatly. Then, the fabricated mask was put on the specimen. Next, the aerosol paint spray was sprayed 30° from the normal to the rubber surface at a distance of 30 cm. The spraying was carried out at all 4 directions to ensure that the paint spray can spread evenly on the specimen surface to create a nice round shape. Since the colour of the rubber specimen is light brownish, black colour markers were created on it as shown in Figure 3.7. The spray paint used is Canbrush non-crack and petrol resistant C30 black spray paint.

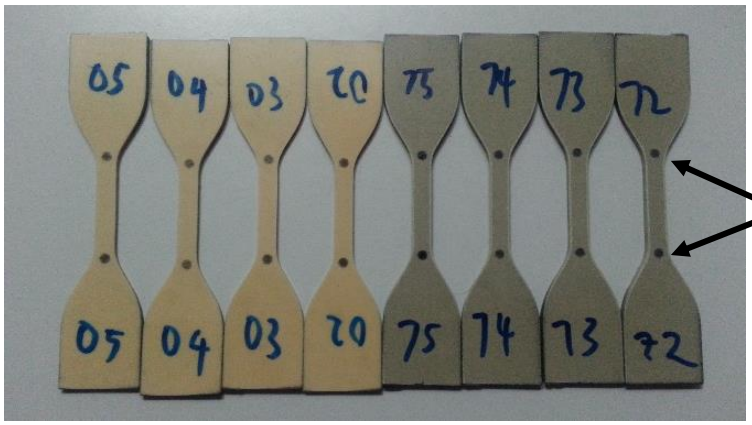

Figure 3.7: The rubber specimens with markers created.

3.4 Preparation of Spacers

Spacers were prepared as they are needed for the validation test. These spacers are used to stretch or apply strain on the rubber specimen. Spacers were cut into different lengths to represent different strains were applied. Seven spacers were cut according to the minimum length of the rubber specimen and maximum length that the flatbed scanner can detect, as shown in Figure 3.8. The spacers were spray painted with black colour to create contrast against the specimens. The lengths of the spacers were measured using coordinate measuring machine (CMM). Firstly, a spacer was placed on the worktable vertically. Then, two planes were created based on the upper surface of the spacer and the surface of the worktable, as shown in Figure 3.9. After that, the distance between the two planes was calculated. The measured lengths of spacers were tabulated in Table 3.1.

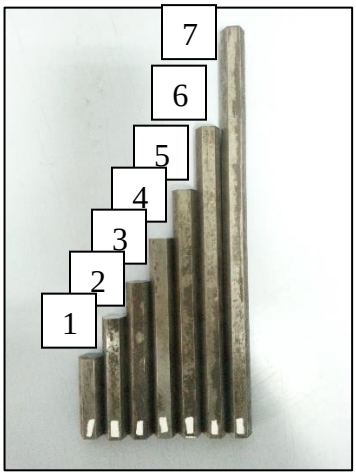

Figure 3.8: Seven spacers were cut for validation test.

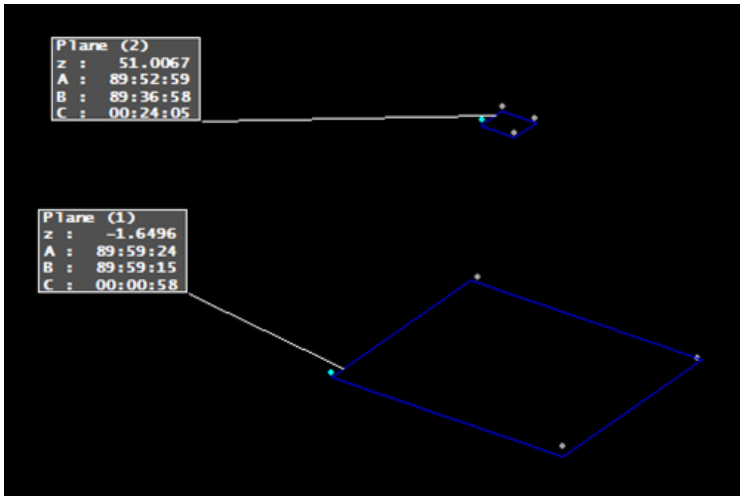

Figure 3.9: Two planes were created and their distance was calculated.

Table 3.1: The length of the spacers

Spacer	Length (mm)
1	52.6563
2	77.2640
3	103.7154
4	126.9170
5	161.3084
6	202.4009
7	265.4830

3.5 Image Acquisition Equipment

Canon Flatbed Scanner model CanoScan 5600F as shown in Figure 3.10 was used as the image acquisition device for this research. The flatbed scanner provides object line scanning with single array of photo sensors by moving scan head under the glass surface. CanoScan 5600F offers a nominal scanning resolution of 600dpi. It also provides large scanning field that can overcome the limited field-of-view of CCD camera when measuring high strain rate polymeric material. There is also built-in lighting system in the scanner to ensure consistent illumination and avoid exposure problem during scanning process. A loading rig that is used to clamp a rubber specimen, which is shown in Figure 3.11, was directly placed

on the frame for support. In addition, a white colour background cardboard was placed on top of the loading rig to cover up the setup. The specifications of CanoScan 5600F scanner are shown in Table 3.2.

Figure 3.10: Canon flatbed scanner model CanoScan 5600F.

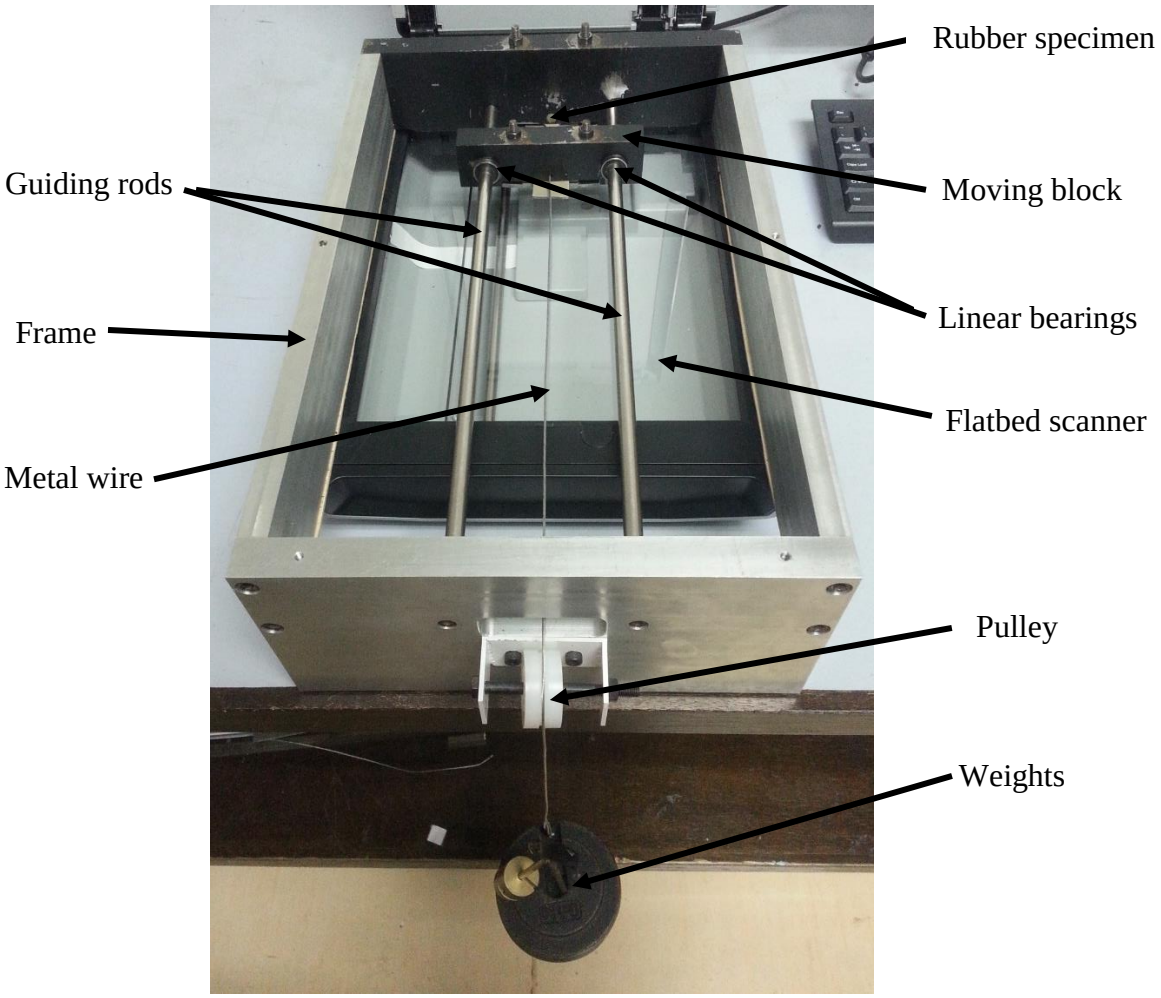

Figure 3.11: The loading rig was placed on the flatbed scanner.

Table 3.2: Specifications of CanoScan 5600F scanner

Sensor Type	CCD 6-line colour
Light Source	White LED/ Cold cathode fluorescent lamp
Optical Resolution	4800 x 9600 dpi
Selectable Resolution	25-19200 dpi (ScanGear)
Scanning Bit Depth (Color)	48 bit input (16 bit input for each color) 48 bit or 24 bit output (16 bit or 8 bit output for each color)
Scanning Speed (Color)	3.7 msec./line (600 dpi)
Maximum Scanning Field	A4/Letter: 216 x 297 mm
Operating Range (Temperature)	10 °C to 35 °C (50 °F to 95 °F)
Power Consumption	In operation: 19 W maximum, Stand-by: 3.2 W *4, Off: 0.4 W *4
Exterior Dimensions (W) x (D) x (H)	272 x 491 x 97 mm
Weight	Approximately 4.3 kg

3.6 Conversion of Unit from Pixel to Millimeter

The measured strain values obtained from MATLAB algorithm were in pixel. Therefore, conversion from pixel to millimeter is required in order to compare the measured strain with applied strain. During the image acquisition, the rubber specimen was scanned at 5 mm above the glass platen to avoid friction between the specimen and glass platen. Therefore, in order to know the conversion value, the standard fixed frequency target with fixed dot spacing, as shown in Figure 3.12, was placed on eight pieces of nuts with 5mm height, as shown in Figure 3.13, and scanned using a nominal resolution of 600 dpi as shown in Figure 3.14.

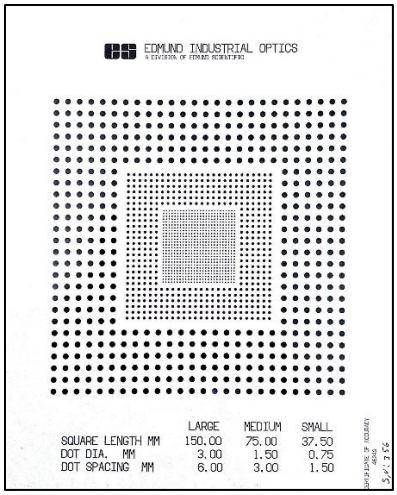

Figure 3.12: The standard fixed frequency target with fixed dot spacing.

Figure 3.13: Eight pieces of nuts with 5mm height.

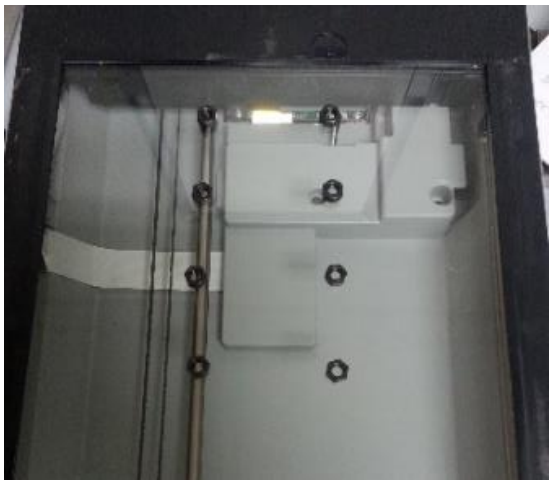

Figure 3.14: Eight pieces of nuts were placed on the glass platen of scanner.

The standard fixed frequency target was placed on the scanner with the large black dots situated at the center of the scanner, which was labelled in red box as shown in Figure 3.15(a). Then, an image was scanned and processed. A manual cropping was carried out to crop only two large black dots and displayed them as shown in Figure 3.15(b). The cropped image was binarized as shown in Figure 3.15(c). In MATLAB, white colour indicates object while black colour indicates background. Therefore, the black and white regions of the image was inverted in order to detect the dots as objects, which was shown in Figure 3.15(d). The centroid of the two dots were determined through 'regionprops' function. The distance between the two dots

were determined by deducting their *y* coordinates. These steps to determine the distance between two centroids were repeated at five different places from the top to bottom of the calibration target. The MATLAB algorithm developed for the conversion from pixel to millimeter can be viewed at Appendix A. The measured distances were recorded and tabulated in Table 3.3. The conversion result shows that the scale factor is 0.0423 mm/pixel.

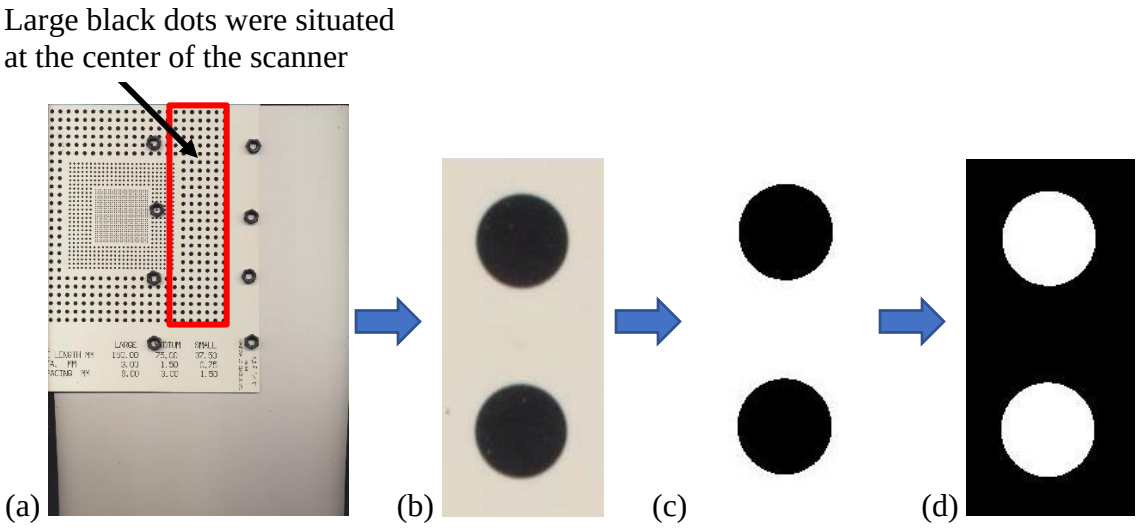

Figure 3.15: (a) The scanned image with standard fixed frequency target. (b)Two dots were manually cropped. (c) The cropped image was binarized. (d) The black and white regions of the image were inverted to detect the two dots as objects.

Table 3.3: Five readings of distance between two centroids of large black dots

Reading	**Distance between two centroids of large dots (pixel)**
1	141.5759
2	141.8288
3	142.0289
4	141.4975
5	141.6396
Average	**141.7141**

3.7 Computation of Applied Strain for Validation Experiment

A validation experiment that will be further explained in Section 3.10 to determine the accuracy of MATLAB algorithm developed in measuring the distance between centroids of markers, the measured strain value will be compared with the applied strain value. Therefore, the applied strain value was calculated. When a force is applied, the strain is the same throughout the specimen. The strain, ε, is given by:

$$\varepsilon = \frac{\Delta L}{L_i} = \frac{L_f - L_i}{L_i}$$

where L_i is the initial length, L_f is the final length and ΔL is the elongation. By comparing the strain at two different areas, it is given by:

$$\frac{PQ_f - PQ_i}{PQ_i} = \frac{AB_f - AB_i}{AB_i}$$

where PQ_i is the inner length of the specimen after being clamped on the loading rig, which is fixed at 42.50 mm, PQ_f is the inner length of the specimen after the strain is applied, which depends on the amount of strain applied, AB_i is the gage length, which is fixed at 33 mm and AB_f is the final gage length after strain is applied. Two images labelled with PQ_i, PQ_f, AB_i and AB_f were shown in Figure 3.16. The expected value of AB_f and applied strain value were calculated and tabulated in Table 3.4.

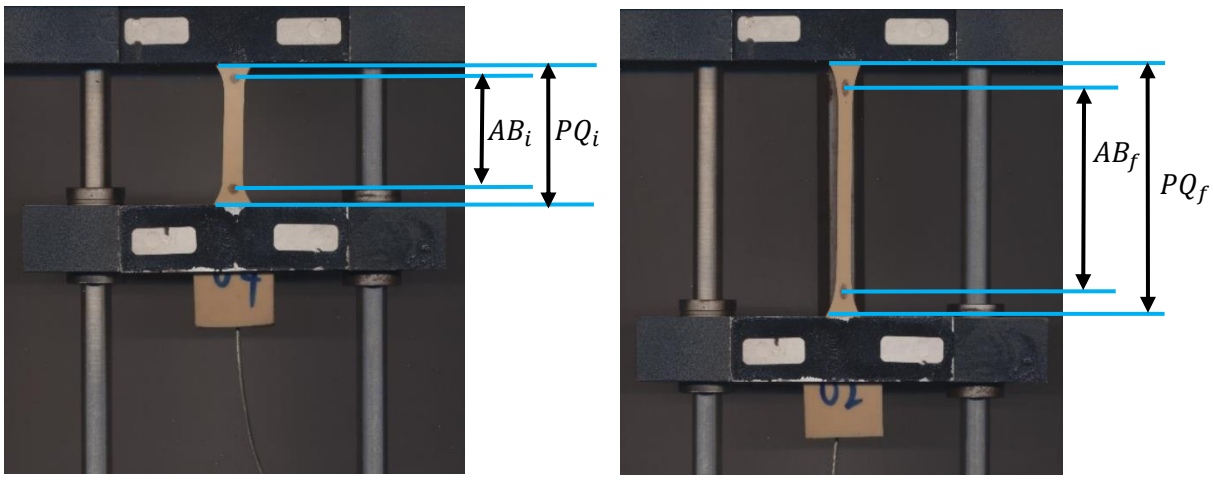

Figure 3.16: (a) The scanned image before strain applied with PQ_i and AB_i labelled. (b) The scanned image after strain applied with PQ_f and AB_f labelled.

Table 3.4: The expected value of AB_f and applied strain of spacer with different lengths

Spacer length, PQ_f (mm)	Expected value of AB_f (mm)	Applied strain, ε
52.6563	40.8668	0.2384
77.2640	59.9932	0.8180
103.7154	80.4941	1.4392
126.9170	98.5473	1.9863
161.3084	125.1923	2.7937
202.4009	157.0844	3.7601
265.4830	206.0428	5.2437

3.8 Tensile Test

Tensile tests were carried out on the five rubber specimens with 0, 10, 30, 50 and 70 phr bentonite loadings. The machine used was Instron 3367 machine. The loading rate was set to 50 mm/min. This tensile test was carried out to determine the maximum load and maximum strain that the specimens can withstand and deform before fracture. The results are useful to determine the optimum constant load or weights that should be applied to all the specimens during the creep test. The process of loading the specimen on the machine, the increasing of load applied until fracture occurred on the specimen were shown in Figure 3.17. All the five specimens were fractured at the end of the tensile tests, which are as shown in Figure 3.18.

3.9 Loading Fixture Setup and Image Acquisition Procedures

The loading fixture for validation test was setup as shown in Figure 3.19. The procedures for setting up are as follow. Firstly, a rubber specimen was placed on the center and parallel to the guiding rods. The rubber specimen was clamped tightly with threaded nuts and leaving only 42.5 mm in between the clamps at two ends. The loading fixture was then placed and aligned on the flatbed scanner. A spacer with length of 52.6563 mm that is used to stretch the specimen was placed in the center too, behind the rubber specimen. A white colour background cardboard was placed on top of the loading rig to enclose it. Then, an image was scanned at the nominal resolution of 600 dpi. This validation test was then repeated by using spacers of different lengths (77.2640, 103.7154, 126.9170, 161.3084, 202.4009, 265.4830 mm).

(a)  (b)  (c) 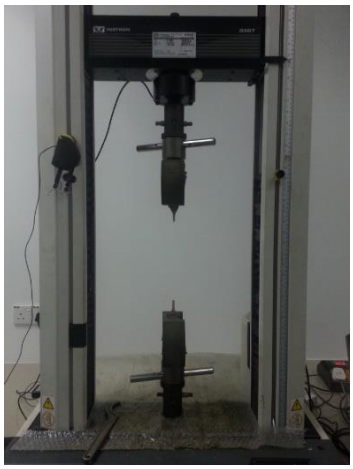

Figure 3.17: (a) The loading of specimen on the clamps of tensile test machine, (b) the increase of load applied on the specimen, (c) fracture occurred on the specimen.

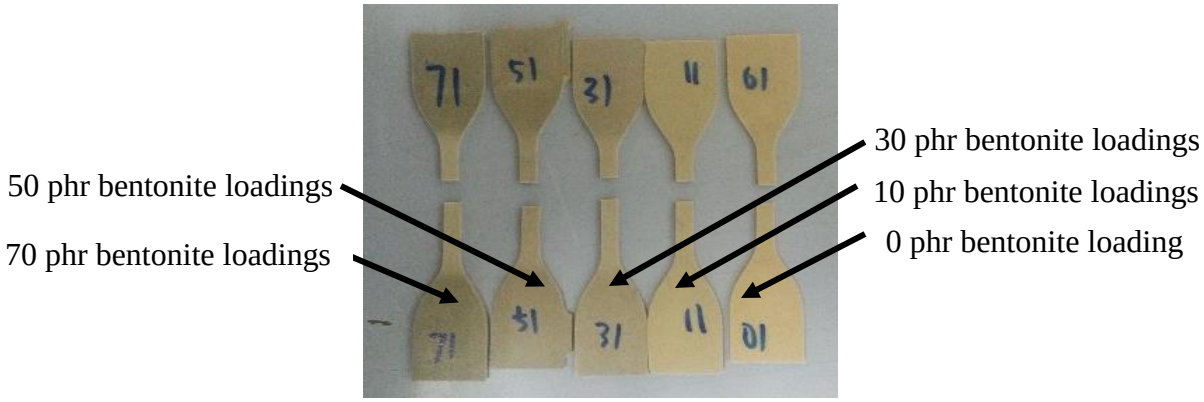

Figure 3.18: All five rubber specimens with 0, 10, 30, 50 and 70 phr bentonite loadings were fractured after tensile test.

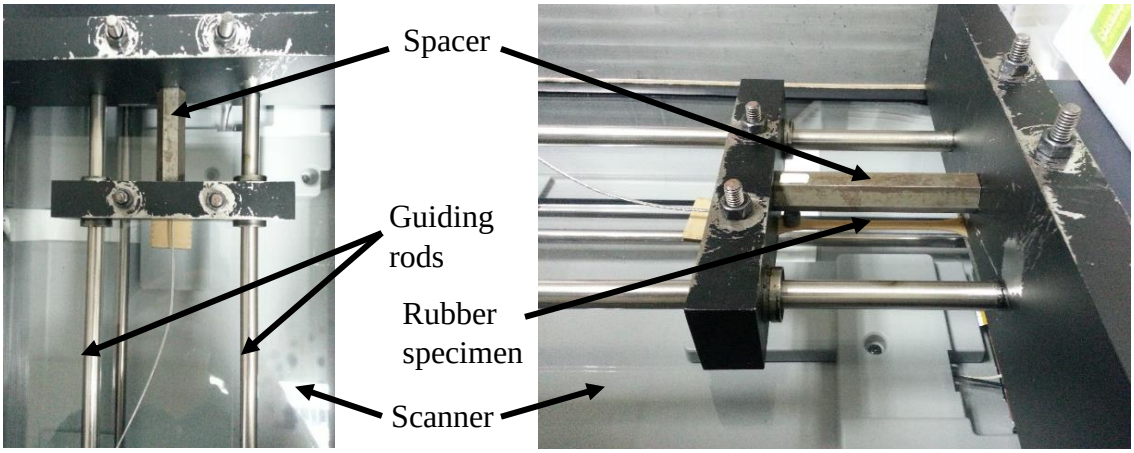

Figure 3.19: The (a) top view and (b) side view of the validation test setup.